Histopathological evaluation of RPL5 expression in triple-negative breast cancer: an integrated immunohistochemical and transcriptomic study

Bing Zhao, Peiyuan Yu, Li Li, Zhenhui Zhao, Xiner Zhang

Department of Breast Cancer, Affiliated Tumor Hospital of Xinjiang Medical University, Urumqi, Xinjiang, China

ABSTRACT

Triple-negative breast cancer (TNBC) is an aggressive subtype of breast cancer characterized by high invasiveness, limited therapeutic options, and unfavorable clinical outcomes. Ribosomal protein L5 (RPL5), a component of the large ribosomal subunit, has been implicated in ribosome biogenesis, translational regulation, and p53-associated cellular processes. This study investigated the immunohistochemical expression pattern of RPL5 in TNBC tissues and explored its potential biological significance through integrated transcriptomic analyses. Tumor tissues from 37 patients with TNBC and 7 adjacent non-tumorous breast tissues were collected from the Affiliated Tumor Hospital of Xinjiang Medical University between December 2017 and December 2023. RPL5 protein expression was evaluated by immunohistochemistry, and its association with clinicopathological characteristics was analyzed. Public transcriptomic datasets from TCGA-BRCA and GEO were further used to validate RPL5 expression patterns in TNBC. Co-expression analysis and Gene Ontology (GO)/Kyoto Encyclopedia of Genes and Genomes (KEGG) enrichment analyses were performed to investigate potential biological functions and signaling pathways associated with RPL5. Immunohistochemical analysis demonstrated significantly lower RPL5 protein expression in TNBC tissues compared with adjacent normal breast tissues (p=0.001). In contrast, transcriptomic analyses revealed significantly higher RPL5 expression in TNBC compared with non-TNBC breast cancer subtypes (p<0.001). No significant associations were observed between RPL5 expression and clinicopathological parameters, including age, tumor size, menopausal status, TNM stage, histological grade, or lymph node metastasis (all p>0.05). Survival analysis showed no significant difference in overall survival between patients with high and low RPL5 expression. Functional enrichment analyses indicated that RPL5-related genes were predominantly involved in ribosome biogenesis, translational regulation, and p53-related signaling pathways. These findings suggest that abnormal RPL5 expression may be associated with TNBC biology through ribosome-related programs, although causal roles require functional validation. RPL5 may represent a potential histopathological and molecular indicator associated with TNBC biology, although its precise functional role requires further experimental validation.

Key words: triple-negative breast cancer; RPL5; immunohistochemistry; ribosome biogenesis; TCGA; transcriptomic analysis; p53 signaling pathway.

Correspondence: Bing Zhao, Department of Breast Cancer, Affiliated Tumor Hospital of Xinjiang Medical University, No.789 Suzhou East Street, Urumqi, Xinjiang 830011, China. E-mail: doctorcrystal@163.com

Contributions: Bing Zhao, conceptualization, funding acquisition, writing original draft preparation. Peiyuan Yu, Li Li, investigation, software, statistical analysis, reviewing and editing. Zhenhui Zhao, Xiner Zhang, reviewing and editing, methodology, supervision. All authors read and approved the final manuscript.

Conflict of interest: the authors declared no conflict of interest.

Availability of data and materials: the data that support the findings of this study are available from the corresponding author upon reasonable request.

Funding: this study was supported by National Natural Science Foundation of China (grant no. 82560554) and Ten-zan's High-level Talent Development Programme in Medicine and Health (grant no. TSYC202301B019).

Introduction

TNBC refers to a subtype of breast cancer characterized by the absence of ER, PR, and HER2, accounting for approximately 15-20% of all breast cancer cases.[1] TNBC is known for its aggressive nature, high risk of recurrence and distant metastasis, and overall poor prognosis. Due to the lack of ER, PR, and HER2 expression, TNBC is not sensitive to endocrine therapy or HER2-targeted therapy, and chemotherapy remains the mainstay of clinical treatment.[1,2] Although immunotherapy and PARP inhibitors have shown some efficacy in certain patients in recent years, the overall benefit remains limited. Therefore, there is an urgent need to explore new molecular markers to aid in diagnosis, evaluate prognosis, and guide personalized treatment.[3,4] RPL5 is a vital part of the large ribosomal subunit, crucial for preserving ribosomal structural integrity and facilitating protein synthesis. Research indicates that RPL5, aside from its traditional ribosomal roles, is crucial in regulating the cell cycle, responding to DNA damage, and activating the p53 signaling pathway, significantly influencing development and progression. Previous studies have suggested that RPL5 is abnormally expressed in multiple malignancies and may influence tumor biological behavior by regulating cell proliferation, apoptosis, and invasion.[5-7] However, the expression characteristics of RPL5 in TNBC and its relationship with clinicopathological parameters and patient prognosis remain underexplored, and its potential molecular mechanisms require further elucidation.

In recent years, the development of bioinformatics technologies has provided powerful tools for studying tumor molecular mechanisms.[8] By integrating transcriptomic data and clinical information from public databases such as The Cancer Genome Atlas (TCGA) and Gene Expression Omnibus (GEO), the expression patterns and prognostic value of candidate genes can be validated in multi-cohort, large-sample contexts. Furthermore, by analyzing co-expression and functional enrichment, one can anticipate the biological processes and signaling pathways these genes could be part of.[9,10] Based on this, the present study combines clinical sample detection and bioinformatics analysis to investigate the expression characteristics of RPL5 in TNBC, its relationship with clinicopathological features and prognosis, and further predict its potential molecular mechanisms. The aim is to provide a theoretical basis for elucidating the biological role of RPL5 in TNBC and its potential clinical application value.

Materials and Methods

Clinical samples and data collection

This study collected tumor tissues from 37 TNBC patients and 7 adjacent normal tissues as controls, treated at the Cancer Hospital Affiliated to Xinjiang Medical University from December 2017 to December 2023. Adjacent non-tumorous tissues (n=7) were collected from available non-lesional areas of the same surgical specimens and were confirmed as non-malignant by routine pathology. All patients signed informed consent forms, and the study was approved by the hospital's ethics committee (K-2024254). The enrolled patients were pathologically confirmed as TNBC after surgery, with adjacent tissues being normal breast tissues. Patients were aged ≥18 years, had complete clinical and pathological data, and were newly diagnosed without prior radiotherapy, chemotherapy, endocrine, or targeted therapy. All patients underwent standard surgical resection (mastectomy or breast-conserving surgery with axillary lymph node dissection/sentinel node biopsy) and received adjuvant chemotherapy according to NCCN guidelines: 32/37 (86.5%) received anthracycline-taxane-based regimens, 3/37 (8.1%) received CMF-like regimens, and 2/37 (5.4%) received platinum-based regimens due to BRCA1/2 mutation status. Adjuvant radiotherapy was administered to 24/37 (64.9%) patients (post-mastectomy chest wall irradiation or breast-conserving radiotherapy). Patients with preoperative distant metastases, recurrence, severe underlying diseases, or male breast cancer were excluded. Clinical and pathological data, including age, menopausal status, maximum tumor diameter, TNM stage, histological grade, and lymph node metastasis status, were collected to provide a data basis for subsequent immunohistochemistry (IHC) detection and clinical correlation analysis.

Immunohistochemistry

Paraffin-embedded tissue blocks were sectioned (4 μm), baked at 60°C for 2 h, deparaffinized in xylene, and rehydrated through a graded ethanol series (100%, 95%, 80%, 70%). Immunohistochemical staining was performed using a rabbit two-step polymer detection system (PV-9001, ZSGB-BIO, Beijing, China). Heat-induced epitope retrieval was performed in pH 8.0 EDTA buffer (ZLI-9069, ZSGB-BIO) using a pressure cooker for 3 min, followed by natural cooling to room temperature and three PBS washes (5 min each). Endogenous peroxidase activity was quenched with 3% hydrogen peroxide solution at room temperature for 30 min, followed by PBS washing. Sections were then incubated with rabbit polyclonal anti-RPL5 primary antibody (1:100 dilution; catalog no. ab157110, Abcam, Cambridge, UK) at 37°C for 1 h, followed by three PBS washes and incubation with the polymer horseradish peroxidase-conjugated secondary antibody (included in PV-9001 kit) for 1 h at room temperature. After PBS washing, DAB chromogen (ZLI-9018, ZSGB-BIO) was applied for approximately 3 min, followed by hematoxylin counterstaining, graded alcohol dehydration, xylene clearing, and neutral balsam mounting. Normal human tonsil tissue was used as a positive control for RPL5, showing expected cytoplasmic and nuclear staining. For negative controls, the primary antibody was replaced with PBS (omission control) and an isotype-matched rabbit IgG (ab27478, 1:100, Abcam) on adjacent sections of TNBC tissue to exclude non-specific binding. No immunoreactivity was observed in negative control sections.

Evaluation and inter-observer agreement: results were interpreted as positive if RPL5 showed coarse granular or patchy yellow to brown staining in the cytoplasm. Two board-certified pathologists (with >10 years of experience in breast pathology) independently evaluated 10 high-power fields (×400 magnification) per section, counting a total of 1,000 epithelial cells. Semi-quantitative scoring was based on staining intensity (0-3 points: 0 = no staining, 1 = weak, 2 = moderate, 3 = strong) and the proportion of positive cells (0-4 points: 0 = 0%, 1 = 1%-25%, 2 = 26%-50%, 3 = 51%-75%, 4 = 76%-100%), with the product of the two scores representing the immunoreactive score (IRS). IRS ≤8 was defined as low expression, and IRS >8 as high expression. Inter-observer agreement was assessed using Cohen's kappa statistic. The initial kappa value was 0.82 (substantial agreement). For the 6 cases (16.2%) with initial discordant scores, the two pathologists reviewed the slides together under a multi-head microscope and reached a consensus through discussion. The final consensus kappa value was 1.00 (perfect agreement).

Bioinformatics analysis

Data sources and download

Public database data used in this study were primarily obtained from the TCGA Breast Cancer Cohort (TCGA-BRCA) and GEO. TCGA-BRCA data were downloaded using the TCGAbiolinks package in R (version 4.2.2), obtaining breast cancer RNA sequencing expression data (HTSeq-FPKM format) and corresponding clinical information. GEO database data were downloaded using the GEO query package, with search keywords "triple negative breast cancer" and "Homo sapiens." Breast cancer datasets containing explicit ER, PR, and HER2 status information were selected for subsequent analysis.

Sample screening and grouping

Based on IHC results, breast cancer samples with negative ER, PR, and HER2 were defined as the TNBC group, while others were classified as the non-TNBC group, with normal breast tissues as controls. In TCGA-BRCA, samples with missing key information or follow-up <30 days were excluded, as well as duplicates or outliers. The final samples were used for differential expression, prognosis, co-expression, and functional enrichment analyses, ensuring comparability among groups and supporting the study of RPL5 in TNBC.

Differential expression analysis

RPL5 expression levels were represented as FPKM values and $\log_2$-transformed ($\log_2$[FPKM+1]) to stabilize variance and normalize distribution. For METABRIC data, pre-processed log□-intensity values were used directly. Wilcoxon rank-sum test was used to compare RPL5 expression differences between tumor tissues and normal breast tissues, TNBC and non-TNBC, and different breast cancer subtypes (*e.g.*, TNBC, HER2-enriched, and Luminal subtypes). Differential analysis was performed using the limma package in R, with a significance level set at $p<0.05$.

Survival analysis

Based on the median level of RPL5 expression, patients were categorized into groups with high and low expression. To ensure robustness of the prognostic findings, sensitivity analyses were additionally performed using: i) the optimal cutoff determined by the surv_cutpoint function in the survminer package, which identifies the expression threshold that maximizes the survival difference between groups; and ii) quartile-based grouping [lowest quartile (Q1) *vs* upper three quartiles (Q2-Q4), and lowest three quartiles (Q1-Q3) *vs* highest quartile (Q4)]. The Kaplan-Meier method was used for plotting overall survival (OS) curves, while the log-rank test was applied to compare survival differences among groups. The Cox proportional hazards model was employed for multivariate analysis to determine if RPL5 expression independently predicts breast cancer prognosis, calculating hazard ratios for each variable. Analyses were conducted in R using packages like survival for survival and Cox regression, survminer for Kaplan-Meier plots, and tidyverse for data processing. Statistical significance was defined as $p<0.05$, with all tests two-sided.

Co-expression gene analysis

In the TCGA-BRCA expression matrix, RPL5 was used as the target gene, and its correlation with other gene expression levels was analyzed. Pearson correlation coefficient was used to assess linear relationships, and the cor.test function in R (v4.2.2) was used to calculate correlation coefficients and *p*-values. Genes with an absolute correlation coefficient ≥0.4 and $p<0.01$ were defined as the RPL5 co-expression gene set, ensuring robust correlations and reducing random interference. The expression matrix was preprocessed for missing values and standardized to ensure calculation accuracy and reproducibility. To address potential confounding by ribosomal gene co-regulation and tumor heterogeneity, we additionally performed the following quality control steps: i) tumor purity adjustment - ESTIMATE algorithm was applied to calculate stromal and immune scores for each TCGA-BRCA sample, and correlation analyses were repeated after stratifying samples by tumor purity (low: <50%, medium: 50-80%, high: >80%); ii) proliferation index evaluation - Spearman correlation between RPL5 expression and MKI67 (a canonical proliferation marker) was assessed to determine whether RPL5 co-expression patterns merely reflected proliferative activity; and iii) ribosomal gene enrichment assessment - the proportion of ribosomal protein genes among the top 50 co-expressed genes was quantified to evaluate the specificity of the RPL5 network beyond generalized ribosomal biogenesis. The constructed co-expression gene set provided a basis for subsequent GO/KEGG functional enrichment and pathway analyses, aiding in the exploration of RPL5's potential regulatory network and molecular mechanisms in breast cancer, and supporting its biological function research in different breast cancer subtypes.

Functional enrichment analysis

The RPL5 co-expression gene set was analyzed using the cluster Profiler package in R (v4.2.2) with the org.Hs.eg.db human gene database for functional enrichment. GO analysis (BP, MF, CC) assessed the biological roles of RPL5-related genes, while KEGG pathway analysis identified potential regulatory pathways. Enrichment significance was assessed using two thresholds: i) a stringent threshold of q-value <0.05 (Benjamini-Hochberg false discovery rate-corrected) to identify robustly enriched pathways; and ii) a nominal significance threshold of uncorrected $p<0.05$ for exploratory interpretation, with q-values explicitly reported to indicate the degree of multiple-testing correction. Results were visualized using dot plots and bar plots, intuitively displaying the significance and gene enrichment levels of each functional category and pathway, providing a basis for elucidating RPL5's potential molecular mechanisms in breast cancer. Results were visualized using dot plots and bar plots, intuitively displaying the significance and gene enrichment levels of each functional category and pathway, providing a basis for elucidating RPL5's potential molecular mechanisms in breast cancer.

Statistical analysis

Study data were analyzed using Statistic Package for Social Science (SPSS) 26.0 (IBM, Armonk, NY, USA). Measurement data were presented as mean ± standard deviation, with independent sample *t*-tests for group comparisons. Count data were shown as frequency and percentage, using chi-square tests for comparisons. Tests were two-sided, with significance at $p<0.05$. Survival analysis utilized the Kaplan-Meier method for overall survival curves, and log-rank tests assessed survival differences, focusing on the impact of RPL5 expression on prognosis.

Results

RPL5 expression in TNBC clinical samples and its relationship with clinicopathological features

Immunohistochemical results showed that RPL5 was primarily

localized in the cytoplasm, with partial nuclear positivity. Quantitative analysis revealed that RPL5 immunoreactive scores were significantly lower in TNBC tumor tissues (median IRS = 6, IQR: 4–9) compared to adjacent normal tissues (median IRS = 10, IQR: 8-11; p=0.001, n = 37 tumor *vs* n = 7 adjacent), indicating reduced RPL5 protein expression in TNBC (Figure 1). This suggests that RPL5 may be abnormally regulated during tumor development, and its cellular localization and expression changes provide a basis for subsequent mechanistic studies.

Among 37 TNBC patients, 49% (n=18) exhibited low RPL5 expression, while 51% (n=19) exhibited high expression. Chi-square test results showed no significant correlation between high RPL5 expression and age (p=0.405), maximum tumor diameter (p=0.898), menopausal status (p=0.134), TNM stage (p=1), histological grade (p=0.362), or lymph node metastasis (p=0.134) (P>0.05), indicating that RPL5 expression levels were not significantly associated with these major clinicopathological features (Table 1). To assess the robustness of these null findings, we per-

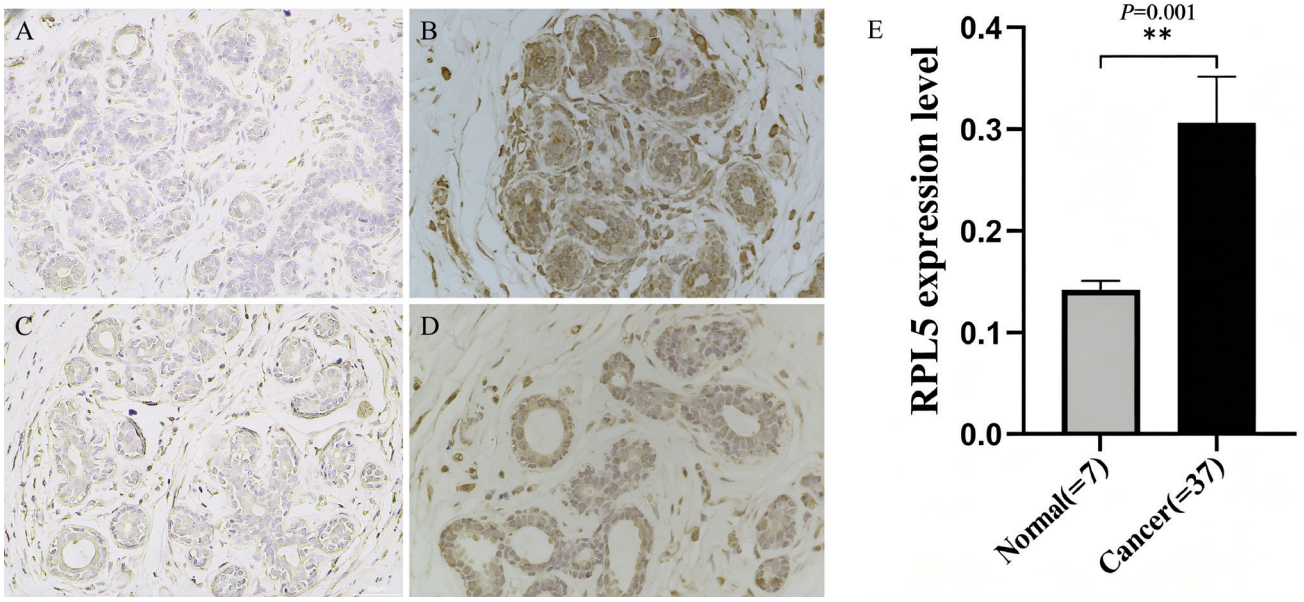

Figure 1. Immunohistochemical results of RPL5 in TNBC clinical samples and adjacent tissues. **A,C**) RPL5 expression in TNBC tumor tissues showing reduced cytoplasmic staining intensity (×400). **B,D**) RPL5 expression in adjacent normal breast tissues showing strong cytoplasmic and nuclear staining (×400). **E**) Quantitative comparison of RPL5 immunoreactive scores (IRS) between TNBC tumor tissues (n=37, median IRS=6, IQR: 4-9) and adjacent normal tissues (n=7, median IRS=10, IQR: 8-11). Mann-Whitney U test, p=0.001. Error bars represent interquartile range. Scale bars: 50 μm.

Table 1. Comparison of RPL5 expression in tumor tissues and clinical characteristics of 37 patients.

Variable	(n=37)	Low (n=18)	High (n=19)	χ^2	p
Age, n(%)				-	0.405
≤60	30 (81.08)	16 (88.89)	14 (73.68)		
>60	7 (18.92)	2 (11.11)	5 (26.32)		
Maximum tumor diameter, n (%)				0.016	0.898
≤2	14 (37.84)	7 (38.89)	7 (36.84)		
>2	23 (62.16)	11 (61.11)	12 (63.16)		
Menopausal status, n (%)				2.245	0.134
No	20 (54.05)	12 (66.67)	8 (42.11)		
Yes	17 (45.95)	6 (33.33)	11 (57.89)		
TNM stage, n (%)				0.785	1
Stage I	6 (16.22)	3 (16.67)	3 (15.79)		
Stage II	23 (62.16)	12 (66.67)	11 (57.89)		
Stage III	5 (13.51)	2 (11.11)	3 (15.79)		
Stage IV	3 (8.11)	1 (5.56)	2 (10.53)		
Histological grade, n (%)				0.833	0.362
Grade 2	13 (35.14)	5 (27.78)	8 (42.11)		
Grade 3	24 (64.86)	13 (72.22)	11 (57.89)		
Lymph node metastasis, n (%)				2.245	0.134
No	20 (54.05)	12 (66.67)	8 (42.11)		
Yes	17 (45.95)	6 (33.33)	11 (57.89)		

formed sensitivity analyses using alternative IRS cutoffs (IRS ≤6 *vs* >6, and IRS ≤4 *vs* >4). The results remained consistent, with no significant associations observed between RPL5 expression and any clinicopathological feature (all $p>0.05$), indicating that the lack of correlation is not an artifact of the specific median cutoff choice. This result suggests that in this study cohort, RPL5 expression status may be independent of traditional clinicopathological parameters, providing a foundation for further exploration of its biological function and potential prognostic value in TNBC. In summary, RPL5 protein is reduced in TNBC relative to adjacent normal tissue, but its intra-tumoral expression level does not stratify patients by conventional severity markers, suggesting that RPL5 may operate through non-canonical biological mechanisms rather than as a surrogate for tumor aggressiveness in this cohort.

Validation of RPL5 expression differences in TCGA and GEO databases

In the TCGA-BRCA cohort, RPL5 expression (log_2[FPKM+1]) was significantly higher in normal breast tissue (n=113, median=5.82, IQR: 5.61-6.04) compared to cancerous tissue (n=1,086, median=5.21, IQR: 4.98-5.45; $p=2.4\times10^{-15}$). Among TNBC samples, RPL5 levels were notably higher in TNBC patients (n=148, median=5.68, IQR: 5.42-5.91) than in non-TNBC patients (n=938, median=5.15, IQR: 4.92-5.38; $p=1.8\times10^{-12}$). Similarly, in the METABRIC cohort, TNBC patients (n=291, median log_2[intensity+1] = 4.95, IQR: 4.72-5.18) exhibited higher RPL5 expression than non-TNBC patients (n=1,707, median=4.62, IQR: 4.38-4.86; $p=0.023$). Within the TCGA-BRCA cohort, RPL5 expression varied significantly across breast cancer subtypes, with the highest levels in TNBC (Kruskal-Wallis $p=3.5\times10^{-14}$; *post-hoc* Dunn test: TNBC *vs* HER2 $p=0.002$, TNBC *vs* Luminal A $p=4.1\times10^{-11}$, TNBC *vs* Luminal B $p=2.8\times10^{-13}$). A similar pattern was seen in the METABRIC dataset, though differences did not reach statistical significance (Kruskal-Wallis $p=0.07$) (Figure 2).

Relationship between RPL5 expression and patient prognosis

In TCGA-BRCA, the median follow-up was 28.3 months with 985 OS events; in the TNBC subgroup, the median follow-up was 24.3 months with 104 OS events. Kaplan-Meier analysis revealed no significant OS difference between high and low RPL5 expression in the TCGA-BRCA cohort ($p=0.46$) and TNBC subgroup ($p=0.77$). The OS difference between TNBC and non-TNBC patients was marginally significant ($p=0.078$). Multivariate Cox analysis identified TNBC subtype [hazard ratio (HR)=3.18, $p=0.0012$] and age (HR=1.06 per year, $p<0.001$) as independent adverse prognostic factors for OS in breast cancer patients (Figure 3 A-C). In contrast, high RPL5 expression (*vs* low expression, HR=0.65, 95% CI: 0.38-1.11, $p=0.115$), HER2 subtype, and tumor stages II/III/IV had no independent significant impact on OS ($p>0.05$, with confidence intervals crossing the null line, Figure 3D). Sensitivity analyses using alternative cutoffs confirmed the robustness of these null findings. With the optimal cutoff identified by surv_cutpoint, RPL5 expression remained non-significantly associated with OS in the overall cohort ($p=0.38$) and TNBC subgroup ($p=0.62$). Similarly, quartile-based comparisons (Q1 *vs* Q2-Q4: $p=0.51$; Q1-Q3 *vs* Q4: $p=0.29$) showed no significant OS differences. These consistent results across multiple grouping strategies indicate that the lack of independent prognostic value for RPL5 is not dependent on the specific cutoff choice.

Co-expression analysis of RPL5

Using Pearson correlation analysis, 261 genes significantly correlated with RPL5 were identified ($|r| \geq 0.4$, $p<0.01$), suggesting that RPL5 may be involved in specific gene regulatory networks in breast cancer. Notably, most of these co-expressed genes were ribosomal protein-related genes, showing a strong positive correlation with RPL5 and reflecting potential functional connections. However, we acknowledge that this high degree of co-regulation may partly reflect generalized ribosomal biogenesis activation

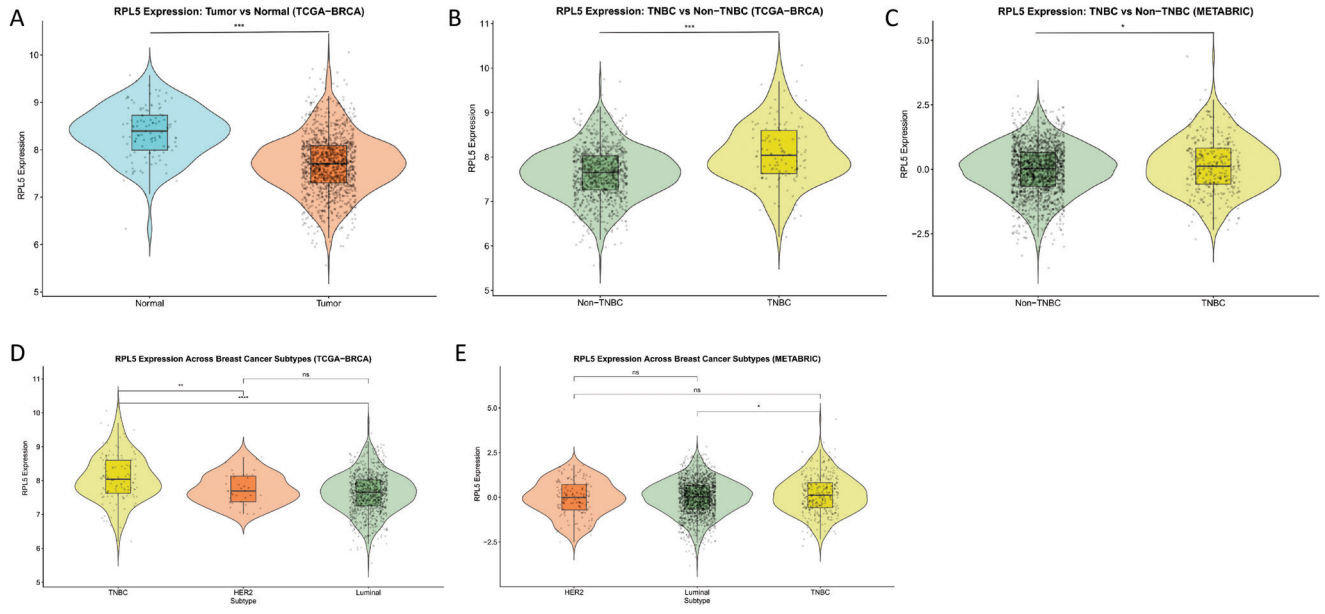

Figure 2. RPL5 expression in breast tissue and molecular subtypes. **A**) Normal vs tumor in TCGA-BRCA. **B**) TNBC *vs* non-TNBC in TCGA-BRCA. **C**) TNBC *vs* non-TNBC in METABRIC. **D-E**) RPL5 expression across subtypes in TCGA-BRCA and METABRIC. Wilcoxon rank-sum test for two-group comparisons; Kruskal-Wallis test for multi-group comparisons (*post-hoc* testing as applicable).

rather than RPL5-specific functions. Supporting this caution, MKI67 expression showed a moderate positive correlation with RPL5 (Spearman r = 0.42, $p<0.001$), indicating that proliferative activity contributes to -but does not fully explain- RPL5 co-expression patterns. Tumor purity stratification revealed consistent RPL5 co-expression profiles across low-, medium-, and high-purity samples (ribosomal genes remained dominant in all strata), suggesting that stromal/immune contamination did not artificially drive the observed correlations. Among the top 50 co-expressed genes, 38 (76%) were ribosomal protein genes, while 12 (24%) were non-ribosomal (including EEF1B2, translation elongation factor), indicating that while ribosomal biogenesis is the predominant theme, a minority of co-expressed genes may represent RPL5-specific regulatory partners. The top ten genes with the strongest correlations were RPS8 (r=0.817), RPL4 (r=0.770), RPS6 (r=0.768), RPL11 (r=0.756), RPS7 (r=0.745), RPS18 (r =0.738), RPL13 (r=0.732), RPS3 (r=0.728), RPL14 (r=0.721), and RPS9 (r=0.715) (Table 2), demonstrating the tight expression pattern linkage between RPL5 and ribosomal protein genes.

To further validate its expression characteristics, the overall expression pattern of these co-expressed genes in TNBC samples was visualized. Heatmap results showed a Spearman correlation coefficient of R = 0.81, $p<0.001$, indicating a consistent high expression state of these RPL5-related genes in TNBC samples (Figure 4). This result not only supports the reliability of Pearson correlation analysis but also suggests that RPL5 and its co-expressed genes may play a synergistic role in ribosome biogenesis and related signaling pathways, providing a solid data foundation for subsequent functional enrichment analysis and molecular mechanism exploration. Overall, the high expression of RPL5 in TNBC and its close co-expression with ribosomal protein genes suggest that RPL5 expression is closely aligned with ribosomal biogenesis-related transcriptional programs in TNBC. Nevertheless, given the inherent co-regulation of ribosomal genes and the moderate correlation with proliferation markers, these findings should be interpreted as descriptive of ribosomal biogenesis activity in TNBC rather than definitive evidence of RPL5-specific oncogenic mechanisms. Functional validation (*e.g.*, RPL5-

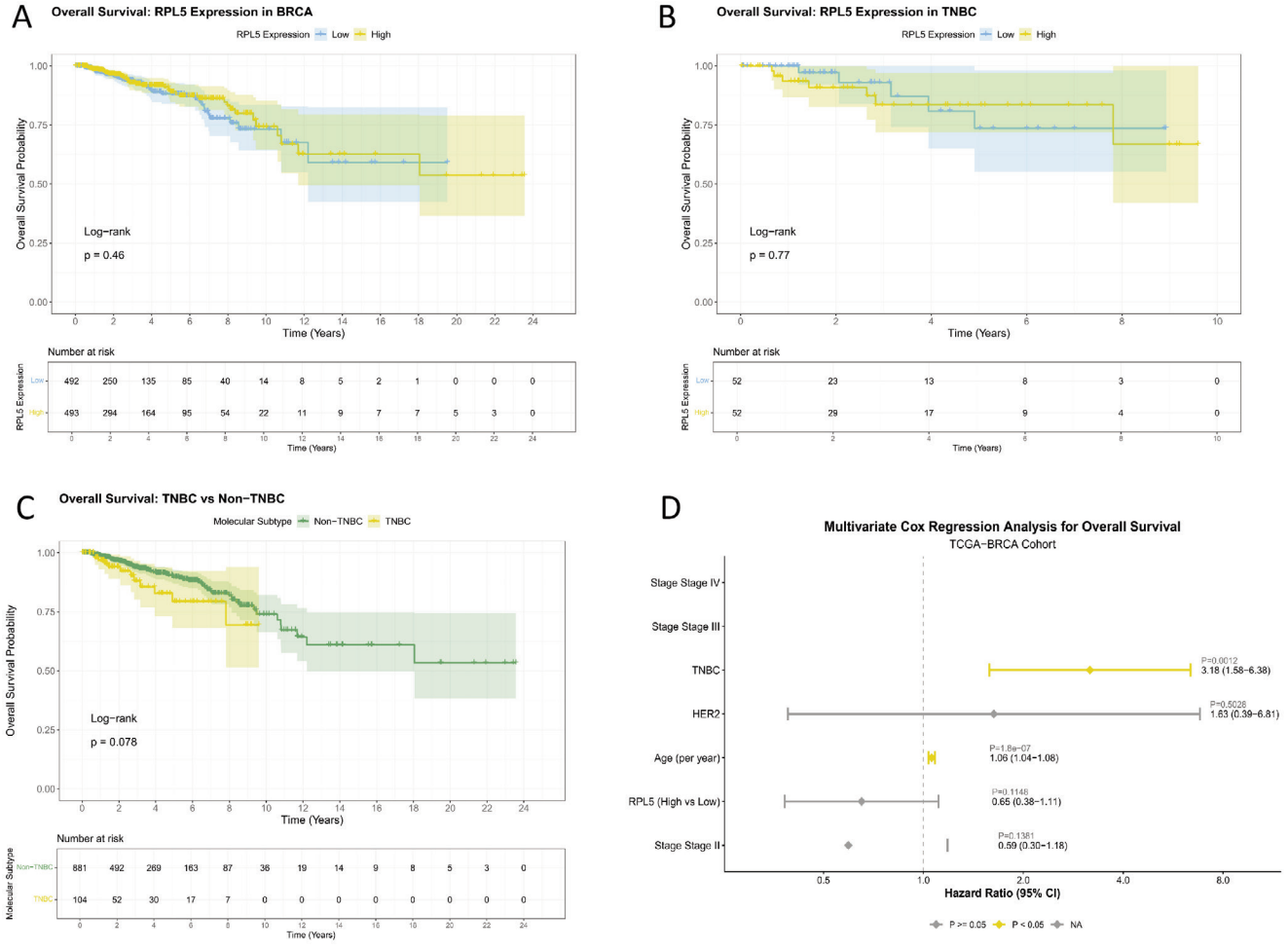

Figure 3. Analysis of RPL5 expression's impact on breast cancer survival. **A**) Overall survival comparison between high and low RPL5 expression in the TCGA-BRCA cohort. **B**) Survival comparison in the TNBC subgroup based on RPL5 expression levels. **C**) Survival comparison between TNBC and non-TNBC patients. **D**) Multivariate Cox regression in TCGA-BRCA, with hazard ratios (HR) on the horizontal axis; HR >1 suggests adverse factors, HR <1 suggests protective factors, and HR =1 indicates no risk difference. Statistical significance is marked in yellow, with specific HR and 95% CI values noted.

specific knockdown with rescue experiments) is required to distinguish specific RPL5 contributions from generalized ribosomal program activation. In summary, RPL5 forms a tightly correlated network with canonical ribosomal proteins in TNBC, reflecting robust ribosomal biogenesis - but whether this represents a specific RPL5-driven regulatory axis or passive coordination by shared transcriptional programs remains to be functionally resolved.

GO and KEGG functional enrichment analysis

GO enrichment analysis of RPL5 co-expressed genes systematically evaluated their functional characteristics from the BP, CC, and MF dimensions. Bar charts and bubble plots visually displayed the differential gene enrichment in each dimension, showing that ribosome-related functional terms were the core enrichment direction, with gene counts and statistical significance (q-value) significantly higher than other functional modules (Figure 5A). Further integration of bar charts summarizing the differential gene enrichment characteristics across the three ontologies revealed that RPL5 co-expressed genes were highly concentrated in ribosome-related pathways, with the CC dimension showing a significantly higher number of enriched genes compared to BP and MF dimensions, indicating that ribosome-related cellular components dominate the RPL5 functional network (Figure 5B). Multi-dimensional circular plots further presented enrichment information from BP, CC, and MF dimensions, visualizing gene counts, enrichment factors (Rich Factor), and statistical significance. Results showed that ribosome-related CC and BP were the main enrichment directions, with extremely high statistical significance (Figure 5C). Hierarchical clustering dendrograms integrating enriched gene counts, Rich Factor, and −log10(*p*-value) information clearly demonstrated the enrichment intensity of the three ontologies. Analysis results showed that ribosome-related CC (*e.g.*, GO:0005840, ribosome), translation-related MF (e.g., GO:0019843, rRNA binding; GO:0003735, translation factor activity), and ribosome biogenesis-related BP *(e.g.,* GO:0042254, ribosomal subunit biogenesis; GO:0006364, rRNA processing) had enrichment factors close to 1 and $-\log_{10}$(*p*-value) greater than 20, indicating that ribosome biogenesis and translational regulation are the core functional modules of the differential genes. Meanwhile, the ubiquitin/p53 signaling pathway appeared as a secondary module in the enrichment analysis, indicating its auxiliary role in the RPL5 regulatory network (Figure 5D). Comprehensive analysis suggests that RPL5 and its co-expressed genes primarily participate in cellular biological processes in TNBC through ribosomal functions and translational regulation, providing a theoretical basis for further exploration of its potential molecular mechanisms.

KEGG pathway enrichment analysis revealed that the ribosome pathway (hsa03010) was significantly enriched after multiple-testing correction (q<0.05), involving 71 genes (GeneRatio = 0.612, $q=2.4\times10^{-15}$). Additionally, several pathways showed nominal significance at uncorrected $p<0.05$ but did not withstand stringent FDR correction (q>0.05), including Protein Processing in the Endoplasmic Reticulum (hsa04141, 4 genes, $p=0.032$, q=0.18), Spliceosome (hsa03040, 4 genes, $p=0.041$, q=0.22), and mRNA Surveillance Pathway (hsa03015, $p=0.038$, q=0.19). Functional categories covered six major classes, including Genetic Information Processing, Metabolism, Human Diseases, and Cellular Processes (Figure 6 A,B). The ribosome pathway showed overwhelming enrichment significance, with both *p*-value and q-value <0.001, which was highly consistent with the core function of ribosome biogenesis identified in GO analysis, validating the central role of the RPL5 co-expression network in protein synthesis. Within the Genetic Information Processing category, pathways such as Protein Processing in the Endoplasmic Reticulum

Table 2. List of RPL5-related genes (Top 20).

Gene	Correlation (r)	*p*
RPS8	0.8173	8.44×10^{-268}
RPL4	0.7705	4.19×10^{-219}
RPS6	0.7686	2.39×10^{-217}
RPL11	0.7517	1.11×10^{-202}
RPS7	0.7477	2.09×10^{-199}
RPS18	0.7464	2.48×10^{-198}
RPL6	0.7360	4.28×10^{-190}
RPL31	0.7339	1.66×10^{-188}
RPL10A	0.7236	8.63×10^{-181}
EEF1B2	0.7162	1.96×10^{-175}
RPS27A	0.7153	8.81×10^{-175}
RPL12	0.7109	9.98×10^{-172}
RPL32	0.6982	3.71×10^{-163}
RPS4X	0.6947	7.06×10^{-161}
RPL3	0.6946	8.18×10^{-161}
RPL37	0.6944	1.10×10^{-160}
RPL35A	0.6923	2.48×10^{-159}
RPL34	0.6890	3.31×10^{-157}
RPL37A	0.6804	7.02×10^{-152}
RPL24	0.8173	8.71×10^{-149}
RPS25	0.7705	8.19×10^{-148}
RPL27A	0.7686	1.12×10^{-147}

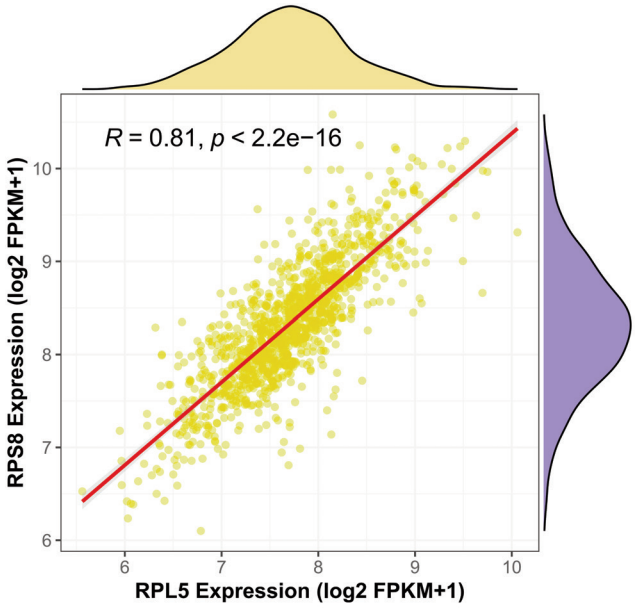

Figure 4. Spearman correlation analysis of RPL5 and RPS8 gene expression. Each dot represents a TCGA-BRCA tumor sample (n=1,086), with the horizontal axis representing RPL5 expression ($\log_2$ (FPKM+1)) and the vertical axis representing RPS8 expression ($\log_2$ (FPKM+1)). The red line represents the linear regression fit, and the gray shaded area indicates the 95% confidence interval. The orange curve at the top and the blue curve on the right represent the marginal density distributions of RPL5 and RPS8 expression levels, respectively.

(hsa04141, 4 genes, p=0.032, q=0.18), Spliceosome (hsa03040, 4 genes, p=0.041, q=0.22), mRNA Surveillance Pathway (hsa03015, p=0.038, q=0.19), and RNA Polymerase (hsa03020, p=0.051, q=0.24) showed nominal enrichment at p<0.05 but did not reach significance after FDR correction (q>0.05). These pathways should be interpreted as suggestive rather than definitive enrichments. Collectively, they suggest that RPL5 co-expressed genes not only participate in ribosomal structural composition but also may engage in mRNA transcription, splicing, quality control, and post-translational protein processing, forming a complete genetic information processing chain. The enrichment of the Protein Processing in the Endoplasmic Reticulum pathway also supports the reported mechanism by which RPL5 induces endoplasmic reticulum stress (ERS) and upregulates GRP78 to inhibit breast cancer cell proliferation. Bar charts further illustrated the number of enriched genes and statistical significance for each pathway, with the ribosome pathway showing absolute dominance in both the number of enriched genes and GeneRatio. Other pathways, such as synaptic vesicle cycle and bacterial invasion of epithelial cells, showed enrichment but had fewer genes, lower GeneRatio, and higher q-values, indicating relatively weaker enrichment reliability. Metabolism-related pathways, such as Cysteine and Methionine Metabolism (hsa00270, p=0.089, q=0.31), Pyruvate Metabolism (hsa00620, p=0.076, q=0.28), Propanoate Metabolism (p=0.112, q=0.35), and Arginine and Proline Metabolism (p=0.095, q=0.33), showed trends toward enrichment but did not reach nominal significance (p>0.05) or withstand FDR correction, suggesting that the RPL5 co-expression network might have ancillary roles in metabolic reprogramming in breast cancer cells.

Hierarchical clustering analysis grouped the pathways into three functional modules: first, the ribosome-centered genetic information processing module, representing the only pathway with robust FDR-corrected significance (q<0.05); second, the nominally significant genetic information processing module, including pathways such as protein processing in the endoplasmic reticulum and spliceosome (nominal p<0.05, q=0.18-0.24); third, the metabolism and stress module, encompassing pathways such as propanoate, pyruvate, and amino acid metabolism, as well as disease-related pathways (nominal p>0.05).; second, the metabolism module, encompassing pathways such as propanoate, pyruvate,

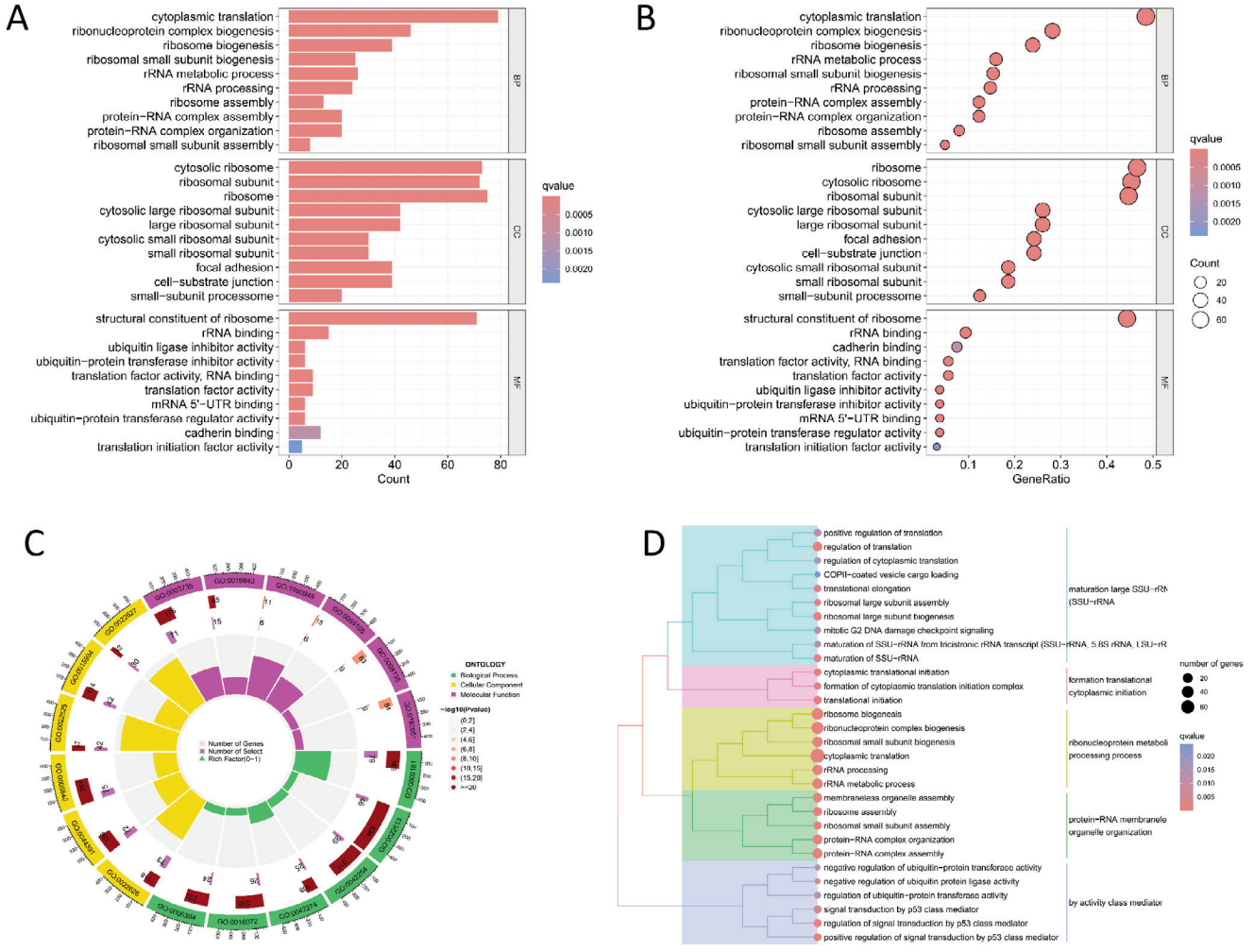

Figure 5. GO enrichment of RPL5 co-expressed genes. **A**) Top enriched GO terms. **B**) Bubble plot of enriched terms across BP/CC/MF. **C**) Circular plot summarizing enrichment. **D**) Clustering of enriched GO categories highlighting ribosome biogenesis/translation-related functions.

and amino acid metabolism, forming a substance metabolism subgroup; third, the disease and stress module, including pathways such as Parkinson's disease and chemical carcinogenesis, involving cellular stress and pathological processes (Figure 6C). This modular functional organization suggests that RPL5 co-expressed genes establish close functional connections between protein synthesis, metabolic regulation, and stress response through interrelated pathway networks. In summary, GO and KEGG analyses converge on ribosome biogenesis as the core functional axis of the RPL5 network, with nominal enrichment in genetic information processing and metabolic pathways - findings that nominate RPL5 as a participant in TNBC translational reprogramming, but do not establish it as an independent node separable from the broader ribosomal apparatus.

Standardized reporting of KEGG enrichment results. We have carefully standardized the reporting of KEGG pathway analysis to distinguish between robustly enriched pathways (FDR-corrected q<0.05) and nominally significant pathways (uncorrected p<0.05). Only the ribosome pathway (hsa03010) met the stringent q<0.05 threshold, confirming it as the core functional axis of the RPL5 co-expression network. Other pathways, while showing nominal p<0.05, did not withstand multiple-testing correction and should be interpreted with caution. This transparent distinction prevents overinterpretation of exploratory findings and aligns with established standards for functional enrichment analysis.

Regarding the cutoff selection for RPL5 expression, we employed a data-driven approach using the median value for both immunohistochemistry (IRS=8) and TCGA (FPKM-based) cohorts. This approach ensures balanced group sizes and minimizes arbitrary threshold selection bias. Importantly, sensitivity analyses using alternative cutoffs -including optimal cutoffs (surv_cutpoint) and quartile-based groupings in the TCGA cohort, as well as alternative IRS thresholds in the IHC cohort- consistently demonstrated no significant associations between RPL5 expression and clinicopathological features or overall survival. These findings reinforce the robustness of our conclusions and suggest that the lack of prognostic significance for RPL5 in TNBC is unlikely to be an artifact of cutoff selection. Nevertheless, we acknowledge that a universally validated cutoff for RPL5 expression has not been established, and future multicenter studies with

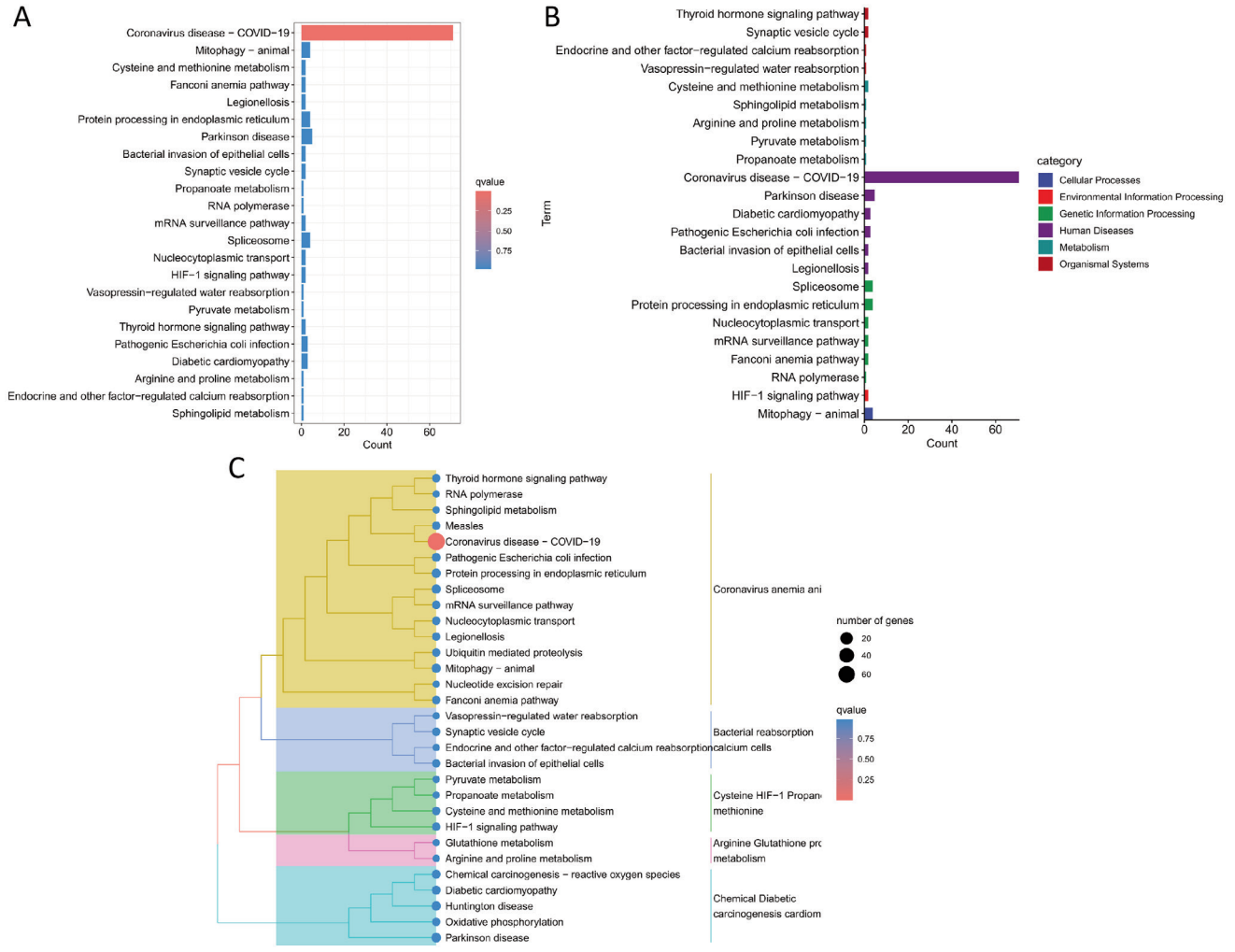

Figure 6. KEGG enrichment of RPL5 co-expressed genes. **A**) Pathway enrichment by gene count and significance. **B**) GeneRatio plot. **C**) Clustering of enriched pathways showing ribosome-centered genetic information processing as the dominant module.

larger sample sizes may help determine the most clinically relevant threshold.

Discussion

This study assessed the expression and clinical significance of RPL5 in triple-negative breast cancer (TNBC) using clinical samples and bioinformatics. RPL5 was found to be highly expressed in TNBC tissues but was not linked to adverse clinical features or prognosis. Validation with TCGA and GEO databases supported these findings, showing RPL5's high expression but not as an independent prognostic factor. The apparent mRNA–protein discrepancy may partly reflect different comparison baselines (TNBC *vs* adjacent normal by IHC, but TNBC vs non-TNBC in transcriptomics) and post-transcriptional regulation affecting translation/protein stability; further validation at the protein level is warranted. RPL5, a key component of the ribosome, is crucial for ribosome stability and protein synthesis and may have roles beyond its traditional functions.[5,7,11] Previous studies have shown that RPL5 is abnormally expressed in various solid tumors, including hepatocellular carcinoma, colorectal cancer, and lung cancer, with its biological functions potentially inhibiting tumors or promoting tumor progression under specific conditions. This suggests that the functions of RPL5 may exhibit heterogeneity across different tumor types and molecular contexts.

Immunohistochemical results in this study showed high cytoplasmic expression of RPL5 in TNBC, suggesting its potential as an auxiliary marker for postoperative pathological evaluation to preliminarily identify high-risk patients.[12,13] Although high RPL5 expression was not directly associated with adverse clinicopathological features or overall survival, its abnormal expression in TNBC still holds biological significance, providing a foundation for subsequent functional studies. If future *in vitro* and *in vivo* experiments confirm the critical role of RPL5 in TNBC cell proliferation, apoptosis, or migration, it may become a novel molecular intervention target, providing a strategic basis for precision therapy.[14,15] Analysis of RPL5 co-expressed genes revealed significant positive correlations with various ribosomal proteins (*e.g.*, RPL11, RPL23, RPS3), and GO functional enrichment analysis indicated that related genes were primarily concentrated in ribosome biogenesis and protein translation processes, suggesting that RPL5 expression is linked to ribosome biogenesis and translation-related processes, which are commonly elevated in highly proliferative tumors; however, whether RPL5 is a driver or a bystander of these programs remains to be determined experimentally.[16-18] KEGG pathway analysis revealed significant enrichment of RPL5-related genes in the p53 signaling pathway, indicating a potential influence on cell cycle and apoptosis via p53 regulation. However, due to the high mutation rate of p53 in TNBC, RPL5's role might shift from tumor-suppressive to tumor-promoting, offering valuable insights for future research.[19-21]

The number of adjacent normal tissues was limited (n=7), which may reduce statistical power and introduce sampling variability. This study has several limitations that may specifically explain the observed discrepancy between significant differential RPL5 expression and the lack of independent prognostic significance. First, the IHC cohort comprised only 37 TNBC patients with relatively short follow-up (median follow-up not reported), providing insufficient statistical power (approximately 30% power to detect a hazard ratio of 0.65 at α=0.05) to identify modest but clinically relevant survival differences. This small sample size also increased the risk of type II error, particularly given the balanced distribution of RPL5 expression (51% high *vs* 49% low), which may have masked a true prognostic effect confined to extreme expression levels. Second, as a single-center retrospective study, selection bias may have been introduced through referral patterns, surgical case mix, or regional demographic factors, potentially limiting the generalizability of the null prognostic finding. The bioinformatics validation, while multi-cohort, relied on retrospectively collected public data with heterogeneous treatment protocols and follow-up schedules, which could dilute subtype-specific prognostic signals. Third, and most critically, the absence of functional experiments prevents interpretation of whether RPL5 overexpression in TNBC represents a driver of tumor progression (which would predict poor prognosis), a compensatory stress response (which would predict no prognostic association), or a passenger effect of enhanced ribosomal biogenesis in rapidly proliferating cells. These mechanistic possibilities have directly opposing prognostic implications that cannot be distinguished by expression correlation alone.

Confounding by ribosomal gene co-regulation and tumor biology. A critical consideration in interpreting our co-expression findings is the inherent co-regulation of ribosomal protein genes, which are frequently transcriptionally coordinated by shared transcription factors (e.g., MYC, TFIIIC) and upstream signaling pathways (mTOR, PI3K/AKT). Consequently, the strong positive correlations between RPL5 and other ribosomal proteins (e.g., RPS8, r=0.817) may partially reflect this global ribosomal biogenesis program rather than protein-specific functional interactions. Furthermore, TNBC is characterized by high proliferative indices and increased ribosomal content, raising the possibility that RPL5 co-expression signatures are confounded by cellularity or proliferation status rather than representing tumor-specific regulatory networks. Our ancillary analyses partially address this concern: the persistence of ribosomal gene dominance across tumor purity strata suggests that stromal contamination is not the primary driver, and the moderate correlation with MKI67 (r=0.42) indicates that proliferation explains only a fraction of RPL5 variance. However, we cannot exclude the possibility that RPL5 overexpression in TNBC is a passive consequence of enhanced translational demand in rapidly dividing cells. Future studies should employ single-cell RNA sequencing to deconvolute tumor versus microenvironment contributions, and perform RPL5-specific perturbation experiments (with non-targeting ribosomal protein controls) to establish causality. Additionally, integrating ribosomal profiling (Ribo-seq) or polysome fractionation could distinguish whether RPL5 co-expression reflects structural ribosomal incorporation versus extraribosomal regulatory functions, which have distinct mechanistic and therapeutic implications. To resolve these limitations and specifically address the differential-expression-versus-prognosis paradox, we propose the following concrete next steps: i) prospective multicenter validation: Expand IHC analysis to ≥200 TNBC cases with standardized follow-up (≥5 years) and centralized pathology review, using quartile-based cutoffs to test whether extreme RPL5 expression (top vs. bottom quartile) predicts prognosis. ii) TP53-stratified functional modeling: given that RPL5 regulates p53 signaling and TP53 is mutated in ~70% of TNBC, perform CRISPR-Cas9-mediated RPL5 knockdown and lentiviral RPL5 overexpression in isogenic TNBC cell lines with defined TP53 status [*e.g.*, MDA-MB-231 (TP53-mutant) *vs* MCF-10A (TP53-wild-type) or CRISPR-corrected isogenic pairs]. Assess proliferation (EdU/MTT), apoptosis (Annexin V/PI), migration (Transwell/wound healing), and tumorigenicity (xenograft) endpoints. This design will directly test whether RPL5's oncogenic or tumor-suppressive function is contingent on TP53 mutational status, potentially explaining why aggregate survival analyses (which

ignore TP53 context) show no significant association. iii) Ribosomal stress and MDM2 axis interrogation: Measure 45S pre-rRNA processing, free RPL5 levels, and MDM2/p53 protein abundance following RPL5 manipulation, to determine whether TNBC-specific RPL5 overexpression disrupts the ribosomal biogenesis checkpoint. iv) Therapeutic targeting feasibility: Evaluate whether RPL5 knockdown sensitizes TNBC cells to cisplatin or PARP inhibitors (*e.g.*, olaparib) in TP53-mutant versus wild-type backgrounds, providing preclinical rationale for RPL5 as a precision target. These integrated experiments will transform our descriptive expression findings into mechanistic and clinically actionable insights.

References

1. Yin L, Duan JJ, Bian XW, Yu SC. Triple-negative breast cancer molecular subtyping and treatment progress. Breast Cancer Res 2020;22:61.
2. Karim AM, Eun Kwon J, Ali T, Jang J, Ullah I, Lee YG, et al. Triple-negative breast cancer: epidemiology, molecular mechanisms, and modern vaccine-based treatment strategies. Biochem Pharmacol 2023;212:115545.
3. Bianchini G, De Angelis C, Licata L, Gianni L. Treatment landscape of triple-negative breast cancer - expanded options, evolving needs. Nat Rev Clin Oncol 2022;19:91-113.
4. Howard FM, Olopade OI. Epidemiology of triple-negative breast cancer: a review. Cancer J 2021;27:8-16.
5. Tong D, Zhang J, Wang X, Li Q, Liu LY, Yang J, et al. MeCP2 facilitates breast cancer growth via promoting ubiquitination-mediated P53 degradation by inhibiting RPL5/RPL11 transcription. Oncogenesis 2020;9:56.
6. Oršolić I, Bursać SAN, Jurada D, Drmić Hofman I, Dembić Z, Bartek J, et al. Cancer-associated mutations in the ribosomal protein L5 gene dysregulate the HDM2/p53-mediated ribosome biogenesis checkpoint. Oncogene 2020;39:3443-57.
7. Xie C, Liang XL, Chen B, Chen S, Xiong FX, Wang QC, et al. hMTR4 promotes p53 protein degradation and tumor growth by accelerating rRNA processing and regulating the RPL5-MDM2 axis. Cell Death Differ 2025;32:2269-83.
8. Liu Y, Sun H, Li X, Liu Q, Zhao Y, Li L, et al. Identification of a three-RNA binding proteins (RBPs) signature predicting prognosis for breast cancer. Front Oncol 2021;11:663556.
9. Xiao R, Chen JY, Liang Z, Luo D, Chen G, Lu ZJ, et al. Pervasive chromatin-RNA binding protein interactions enable RNA-based regulation of transcription. Cell 2019;178:107-21.
10. Perez-Perri JI, Noerenberg M, Kamel W, Lenz CE, Mohammed S, Hentze MW, et al. Global analysis of RNA-binding protein dynamics by comparative and enhanced RNA interactome capture. Nat Protoc 2021;16:27-60.
11. Ma X, Li Y, Zhao B. Ribosomal protein L5 (RPL5)/ E2F transcription factor 1 (E2F1) signaling suppresses breast cancer progression via regulating endoplasmic reticulum stress and autophagy. Bioengineered 2022;13:8076-86.
12. Fancello L, Kampen KR, Hofman IJF, Verbeeck J, De Keersmaecker K. The ribosomal protein gene RPL5 is a haploinsufficient tumor suppressor in multiple cancer types. Oncotarget 2017;8:14462-78.
13. Ren Y, Tao C, Wang X, Ju Y. Identification of RPL5 and RPL10 as novel diagnostic biomarkers of Atypical teratoid/rhabdoid tumors. Cancer Cell Int 2018;18:190.
14. Ivarsdottir EV, Gudmundsson J, Tragante V, Sveinbjornsson G, Kristmundsdottir S, Stacey SN, et al. Gene-based burden tests of rare germline variants identify six cancer susceptibility genes. Nat Genet 2024;56:2422-33.
15. Bi G, Liang J, Bian Y, Shan G, Huang Y, Lu T, et al. Polyamine-mediated ferroptosis amplification acts as a targetable vulnerability in cancer. Nat Commun 2024;15:2461.
16. Hu J, Huang H, Xi Z, Ma S, Ming J, Dong F, et al. LncRNA SEMA3B-AS1 inhibits breast cancer progression by targeting miR-3940/KLLN axis. Cell Death Dis 2022;13:800.
17. Castro-Rivera E, Ran S, Thorpe P, Minna JD. Semaphorin 3B (SEMA3B) induces apoptosis in lung and breast cancer, whereas VEGF165 antagonizes this effect. P Natl Acad Sci USA 2004;101:11432-7.
18. Exposito F, Redrado M, Serrano D, Calabuig-Fariñas S, Bao-Caamano A, Gallach S, et al. G9a/DNMT1 co-targeting inhibits non-small cell lung cancer growth and reprograms tumor cells to respond to cancer-drugs through SCARA5 and AOX1. Cell Death Dis 2024;15:787.
19. Zhou Y, Zhang T, Wang S, Yang R, Jiao Z, Lu K, et al. Targeting of HBP1/TIMP3 axis as a novel strategy against breast cancer. Pharmacol Res 2023;194:106846.
20. Worley BL, Kim YS, Mardini J, Zaman R, Leon KE, Vallur PG, et al. GPx3 supports ovarian cancer progression by manipulating the extracellular redox environment. Redox Biol 2019;25:101051.
21. Lou W, Ding B, Wang S, Fu P. Overexpression of GPX3, a potential biomarker for diagnosis and prognosis of breast cancer, inhibits progression of breast cancer cells in vitro. Cancer Cell Int 2020;20:378.

Received: 19 May 2026. Accepted: 12 June 2026.

Licensee PAGEPress, Italy
European Journal of Histochemistry 2026; 70:4575
doi:10.4081/ejh.2025.4575